Colloids and Surfaces B: Biointerfaces 175 (2019) 1–9

Contents lists available at ScienceDirect

Colloids and Surfaces B: Biointerfaces

journal homepage: www.elsevier.com/locate/colsurfb

Novel grafted electrochemical interface for covalent glucose oxidase immobilization using reactive pentafluorophenyl methacrylate

Margalida Artigues[a], Sejin Oh[b], Joan Gilabert-Porres[b,1], Jordi Abellà[a], Salvador Borrós[b,c], Sergi Colominas[a,*]

[a] Electrochemical Methods Laboratory - Analytical and Applied Chemistry Department at Institut Químic de Sarrià, Universitat Ramon Llull, Via Augusta, 390, 08017, Barcelona, Spain
[b] Grup d'Enginyeria de Materials (GEMAT) at Institut Químic de Sarrià, Universitat Ramon Llull, Via Augusta, 390, 08017, Barcelona, Spain
[c] CIBER-BBN, Networking Center on Bioengineering, Biomaterials and Nanomedicine, Zaragoza, Spain

ARTICLE INFO

Keywords:
Electrochemical biosensor
Plasma modification
Hydroxyethyl methacrylate (HEMA)
QCM-D
Glucose oxidase
Surface engineering

ABSTRACT

One of the most important factors for the proper functioning of enzymatic electrochemical biosensors is the enzyme immobilization strategy. In this work, glucose oxidase was covalently immobilized using pentafluorophenyl methacrylate (PFM) by applying two different surface modification techniques (plasma polymerization and plasma-grafting). The grafted surface was specifically designed to covalently anchor enzyme molecules. It was observed using QCM-D measurements the PFM plasma-grafted surfaces were able to retain a higher number of active enzyme molecules than the PFM polymerized surfaces. An amperometric glucose biosensor using titanium dioxide nanotubes array (TiO_2NTAs) modified by PFM plasma-grafted surface was prepared. The resulting biosensor exhibited a fast response and short analysis time (approximately eight minutes per sample). Moreover, this biosensor achieved high sensitivity (9.76 $\mu A\,mM^{-1}$) with a linear range from 0.25 to 1.49 mM and a limit of detection (LOD) equal to 0.10 mM of glucose. In addition, the glucose content of 16 different food samples was successfully measured using the developed biosensor. The obtained results were compared with the respective HPLC value and a deviation smaller than 10% was obtained in all the cases. Therefore, the biosensor was able to overcome all possible interferences in the selected samples/matrices.

1. Introduction

In last few decades, electrochemical biosensors have been widely explored in many different fields, such as clinical [1], biotechnological [2], food [3] and pharmaceutical [4]. This type of device is the object of attention because it allows for analysis with high specificity, sensitivity, selectivity and low response [5]. Based on their operating principle, electrochemical biosensors are classified as conductimetric, potentiometric and amperometric [6]. Conductimetric devices have been used to determine a change of conductivity as a result of an enzymatic reaction, for example to determine nitrate in water using nitrate reductase [7] or to determine arginine using urease and arginase [8]. On the other hand, potentiometric biosensors generally rely on ion selective electrodes (ISE), for example for the determination of urea with a selective electrode of NH_4^+ cations [9], to determine total phenols in honey [10] or to determine Pb in milk [11]. Finally, amperometric biosensors are the most commonly used because they are quite sensitive and more suited for mass production than the potentiometric and conductimetric ones [12]. Amperometric biosensors have been used to determine a wide range of different analytes, such as bisphenol A [13], amino acids [14], lactose [15], *Salmonella* sp. [16] or the neurotransmitter acetylcholine [17]. Usually, electrochemical biosensors use enzymes as biological recognition element [6]. Among all the available enzymes for industrial applications, glucose oxidase (GOx) is one of the most used. Since the first enzyme electrode for glucose determination was developed by Clark and Lyons in 1962 [18], important progress has been made both in technology and applications of biosensors with innovative approaches involving electrochemistry, nanotechnology and

Abbreviations: D, dissipation; f, frequency; EGDA, ethylene glycol diacetate; FAD, Flavin adenine dinucleotide; GOx, glucose oxidase; HEMA, 2-hydroxyethyl methacrylate; MG, molten globule state; PBS, phosphate buffer solution; PFM, pentafluorophenyl methacrylate; PMG, pre-molten globule state; PS, polystyrene; QCM-D, quartz crystal microbalance with dissipation; SDS, sodium dodecyl sulfate

* Corresponding author.
E-mail address: sergi.colominas@iqs.edu (S. Colominas).
[1] Present Address: Tractivus SL, Via Augusta, 394. 08017 Barcelona, Spain.

https://doi.org/10.1016/j.colsurfb.2018.11.076
Received 29 June 2018; Received in revised form 24 October 2018; Accepted 27 November 2018
Available online 28 November 2018

bioelectronics [19]. Most efforts focus on improving sensitivity, long-term stability and architecture of the developed biosensors. One of the proposed approaches to improve sensitivity consists on directly transferring the electrons from glucose to the electrode through the active site of the enzyme [20]. It is worth mentioning that the FAD cofactor in GOx is profoundly hidden below the protein surface. Thus, extensive research is being performed to wiring the active site of glucose oxidase to the electrode surface [21–24]. On the other hand, recent investigations are centered in devices miniaturization [25–28]. Miniaturization allows to reduce the amount of sample required and the integration of multiple biosensors in arrays in order to increase the throughput and to diminish interference effects. Another hotspot in recent years is to obtain wearable and non-invasive biosensors for real-time monitoring of analytes in sweat, tears or saliva as indicators of a wearer's health status [29–31]. This type of biosensors combined with new communication technologies, such as smartphones or tablets, allow to obtain easy-to-use devices and easy-to-read measurements [32–34]. Despite all the progress made in recent years, developed biosensors still present some technical drawbacks that must be overcome, such as low sensitivity or poor stability.

A key parameter for the proper functioning of electrochemical biosensors is the correct enzyme immobilization on the electrode surface [35]. Immobilization must be done in a way that maintains the structure and the spatial orientation of the protein. In addition, substrate and product, have to be able to diffuse to/from the active site [36], where the biological reaction takes place. The main problem of electrochemical biosensors is the accessibility of the active site of the enzyme, which in most cases is deeply buried in the protein envelopment [6,37]. This is the case of glucose oxidase and its FAD cofactor [38,39]. Thus, an important goal in GOx immobilization is to provide intimate contact between FAD and the sensing surface. To achieve this objective, covalent attachment of enzymes using pentafluorophenyl methacrylate (PFM) has been proposed. PFM offers a highly reactive ester group that can potentially be used to react with the amino groups [40] and it has been previously used to obtain smart, bioactive surfaces which allows aminated bioreceptors immobilization [41]. For example, it was used to covalently immobilize DNA onto carbon nanotubes [42], for BSA monolayers immobilization [43] and to obtain modified bioactive surfaces able to reprogram murine somatic cells into pluripotent cells at high efficiency [44]. Thus, ultra-thin films of plasma-polymerized PFM can be used to covalently immobilized amino-group containing reagents [45], such as GOx. Using this immobilization technique, enzyme molecules are located near the electrode surface leading easy electron transfer. In addition, covalent immobilization avoids enzyme loss at the electrode surface.

In the present work, we report on the construction of a novel and versatile electrochemical platform that can be used for biosensing applications. This platform consists of a PFM surface grafted onto tailored hydrogel coated titanium dioxide nanotubes array (TiO_2NTAs). The high surface area of nanomaterials allows for immobilization of a large number of enzyme molecules, significantly increasing the sensitivity of the sensor [46]. Among all nanomaterials, TiO_2NTAs is one of the most interesting material in recent investigations due to the facility to control its morphology, in addition to its biocompatibility and ability to promote charge transfer processes [47,48]. All these properties make this material suitable as an electrochemical interface [49–52]. The proposed grafted surface is specifically designed to covalently anchor enzyme molecules, via amide bond formation [53,54]. Moreover, the hydrogel thin layer protects the interface from interfering substances allowing the analytes to reach the electrode. GOx was used to demonstrate the high analytical potential of the constructed electrochemical platform.

2. Experimental section

2.1. Materials

Titanium (99.7%, 5 mm diameter) was supplied by Alfa Aesar. PFM was supplied by Apollo Scientific. Argon 5.0 was supplied by Carburos Metálicos. Deconex 11 was supplied by Panreac. Ethylene glycol diacrylate (EGDA) were supplied by Polysciences. GOx type VII from *Aspergillus niger* (100 units/mg), low molecular weight chitosan, hydroxyethyl methacrylate (HEMA), Hellmanex II and sodium dodecyl sulfate (SDS) were supplied by Sigma Aldrich. All the solutions were prepared in ultrapure water. Glucose oxidase was diluted in 0.1 M phosphate buffer solution (PBS) at pH 7.0.

2.2. Surface plasma modifications

Surface modifications were performed in the stainless steel bell-jar plasma reactor described in a previous work [55].

2.2.1. PFM plasma-polymerizations [17]

The monomer (PFM) flask was opened until pressure was reached between $3{\cdot}10^{-2}$ and $5{\cdot}10^{-2}$ mbar. A continuous radio frequency power was fixed at 15 W and pulsed plasma polymerization (duty cycle 10/20) was carried out for 5 min. Plasma discharge was turned off and the PFM vapor flow was kept constant for 5 min more.

2.2.2. HEMA-co-EGDA plasma-polymerizations

The cross-linker (EGDA) flask was opened at pressure reaching $1.2{\cdot}10^{-2}$ mbar. Then, the monomer (HEMA) flask was opened at pressure reaching $3.6{\cdot}10^{-2}$ mbar. A continuous radio frequency power was fixed at 20 W and pulsed plasma polymerization (duty cycle 2/22) was carried out for 10 min. Plasma discharge was turned off and the HEMA/EGDA vapor flow was kept constant for 10 min more.

2.2.3. PFM plasma grafting [43]

Polystyrene sensors and HEMA-co-EGDA coated sensors were activated by argon plasma (pressure between $1{\cdot}10^{-1}$ and $1.5{\cdot}10^{-1}$ mbar). A continuous radio frequency power was set at 15 W and carried out for 15 min. Plasma was turned off and the argon gas line was closed. Then, PFM monomer flask was opened until pressure reaching $7.7{\cdot}10^{-2}$ mbar for 15 min.

2.3. Quartz crystal microbalance with dissipation (QCM-D)

Immobilization process of GOx was characterized using a Q-Sense E1 instrument (Q-Sense AB). The QCM-D sensors used were piezoelectric AT-cut quartz crystal with a fundamental frequency of 4.95 MHz, ones with a polystyrene layer spin-coated on gold (QSX305, Q-Sense AB) and others with a titanium layer (QSX310, Q-Sense AB). All experiments were conducted at room temperature using a flow rate of 50 $\mu L{\cdot}min^{-1}$ in flow mode. 3rd, 5th, 7th, 9th, 11th and 13th overtones were recorded. All solutions were degassed before measurement.

2.4. Biosensor preparation

TiO_2NTAs were synthesized onto Ti substrates by anodic oxidation [56]. A thin film of HEMA-co-EGDA was polymerized onto the Ti/TiO_2NTAs electrode and PFM plasma-grafting was carried out, as described before. Then, 20 μL of GOx solution (15 mg/500 μL) were deposited onto the modified electrode and kept at 4 °C for 24 h. Finally, 20 μL of 0.5% Chitosan solution was deposited and dried with an air stream.

2.5. Glucose determination in food samples

Samples for amperometric biosensor measurements did not need

further preparations than dilution. For the soft drinks and the soy sauces, an adequate volume of the sample was directly added to the measuring chamber, containing 100 mL of 0.1 M PBS (pH 7.0). Dairy products and tomato sauces were first diluted into 50 mL of water. All samples were quantified by the standard additions' method; an adequate volume of sample was added to the electrochemical cell, then 2 additions of 0.25 mM glucose were made. Amperometric measurements were performed in a standard three-electrode configuration by applying -0.4 V vs Ag/AgCl/3 M KCl. The working electrode was mounted in a rotating disc electrode system EG&G PARC model 616.

HPLC is a commonly used method for glucose determination in food samples [57–62]. For this reason, glucose was also determined by HPLC using an Agilent Technologies 1200 Series Chromatograph. Separation was done using a Kromasil® 100 NH_2 column with 5 µm of particle size, 250 x 4 mm. The column was thermostated at 30 °C. Elution was done with 75% acetonitrile in ultrapure water in a single pump system at 1 mL min^{-1}. Eluted components were detected using a refraction index detector (Agilent G1362 A) set at 35 °C. Injection volume was 5 µL and quantification was done by direct interpolation in calibration curve. Soft drink samples for the HPLC analysis were prepared by diluting 10 mL into 100 mL of ultrapure water and then were filtered through 0.45 µm nylon filters. Dairy products, soy and tomato sauces were prepared by dissolving an adequate amount of sample into 50 mL of Milli-Q water, followed by 10 min ultrasonication. The resulting mixture was centrifuged at 5000 rpm for 10 min. The supernatant solutions were filtered through 0.22 µm filters prior to injection.

3. Results and discussion

3.1. Protein immobilization

As it has been stated, the purpose of this work was to develop an electrochemical platform for covalent immobilization of enzymes, maintaining its maximum biological activity. To achieve this goal, PFM was used as enzyme anchor. The amide bond formation between PFM and amine groups (enzymes) is demonstrated in previous studies [40,45,53,54]. PFM was deposited onto the electrode surfaces by plasma-polymerization and by plasma-grafting. These modification techniques were compared using a widely known enzyme such as GOx. The adsorbed mass and the viscoelastic properties of the obtained films were analyzed using QCM-D. In a first set of experiments, polystyrene (PS) sensors were used to study the influence of both modification techniques on the enzyme immobilization process. Plasma polymerization leads to a homogeneous PFM film (ppPFM) while plasma-grafting allows to obtain a less hydrophobic grafted PFM (pgPFM) surfaces. The frequency and dissipation profiles obtained for each modified surface can be seen in Fig. 1.

Fig. 1 shows changes in both frequency (f) and dissipation (D) recorded for each surface. First, a baseline was measured with PBS to stabilize the surface of the sensor's crystal. Then, GOx solution (0.2 mg mL^{-1}) was introduced in the flow module. In all the cases, the frequency rapidly decreased and was stabilized between −20 Hz and −25 Hz. Thus, the adsorbed mass increases indicating an interaction between GOx molecules and the surface. Then, a cleaning step was carried out with SDS and PBS to remove the unbounded protein and frequency profiles varied as a function of the surface. For PS (Fig. 1.A), an increase of the frequency signal was obtained, it returned to the baseline value, indicating that the protein adsorbed mass was eliminated. Conversely, for ppPFM (Fig. 1.B) and for pgPFM (Fig. 1.C), the frequency signals decreased with the SDS cleaning step, indicating an increase of the adsorbed mass. This fact can be related to the formation of a complex due to SDS and GOx interaction [63]. SDS complexes cannot be removed from the electrode surface because of the covalent interaction between PFM and the surface. When PBS was pumped to return to the initial conditions, the frequency signal was stabilized around −11 Hz for the ppPFM film (Fig. 1.B) and around −18 Hz for

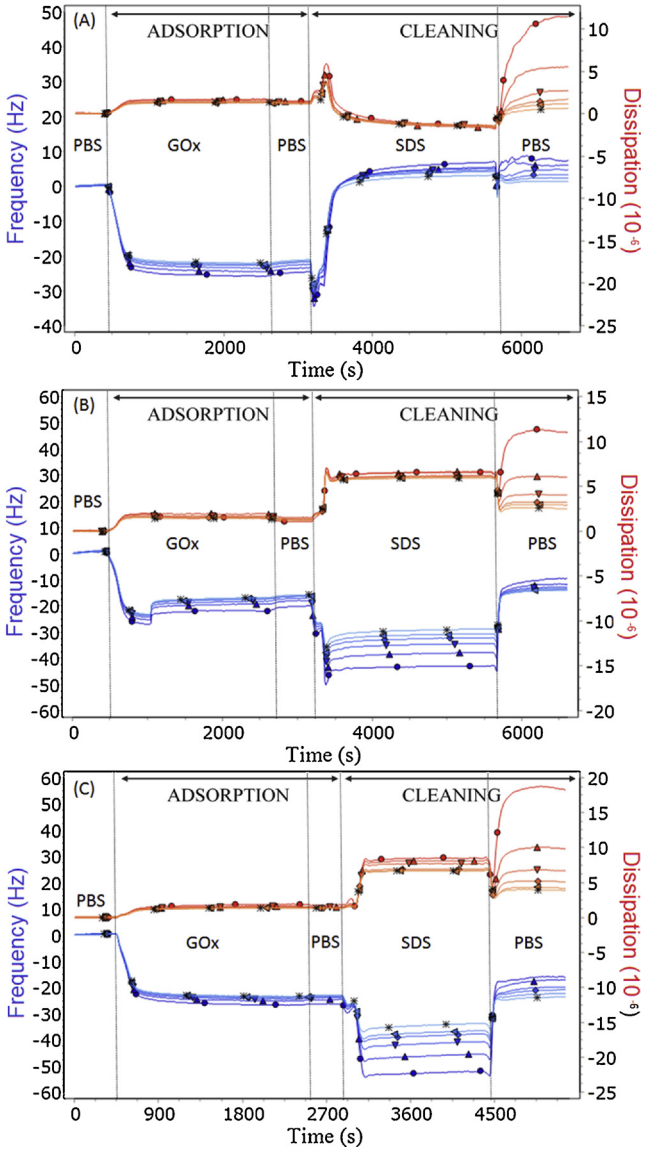

Fig. 1. Frequency (blue line) and dissipation (red line) changes with time for QCM-D monitoring of GOx immobilization and subsequent PBS and SDS cleaning on three types of surfaces: polystyrene (A), polymerized film of PFM (B) and plasma-grafted PFM (C). The 3rd (●), 5th (▲), 7th (▼), 9th (♦), 11th (◄) and 13th (⁎) overtones are shown (For interpretation of the references to colour in this figure legend, the reader is referred to the web version of this article).

the pgPFM film (Fig. 1.C), indicating a covalent interaction between GOx molecules and electrode surfaces. The higher the final frequency value, the higher the retained mass should be. Therefore, higher amount of GOx was retained on the pgPFM surface (see section 3.3).

The dissipation signals recorded for each studied surface are also shown in Fig. 1. Before the SDS interaction, a small variation in the overtones' separation was obtained in all the cases, indicating that a rigid protein monolayer is formed [64]. In contrast, after SDS interaction a variation of the overtones' separation was recorded, being this variation more pronounced with the final PBS cleaning. Thus, after the cleaning step the protein layer was modified, its swelling capability increased due to a change of the buffer pH (5 for SDS and 7 for PBS). As function of the pH, GOx follows a folding/unfolding pathway that affects its conformational state [65]. The native (N) globular dimeric form is stable at pH 7.0. However, at pH more acidic than 6.0 the protein changes into an intermediate conformation [66,67], that can be

the molten globule (MG) or the pre-molten globule (PMG) states [68,69]. Therefore, after each change in pH, GOx molecules suffered conformational modifications that were reflected in the overtones separation.

3.2. Characterization of the protein layer

In order to characterize the protein layer, the dissipation variation (ΔD) versus the frequency shift (Δf) was studied [70]. This relationship provides information not only about the viscoelastic properties of the adsorbed film but also about the resulting conformation of the immobilized protein. The slope of the ΔD/Δf correlation was slightly higher for the ppPFM surface (0.075 Hz^{-1}) than for the pgPFM surface (0.035 Hz^{-1}), indicating that the GOx/ppPFM film is relatively less rigid than the GOx/pgPFM film. Flexible conformations are commonly associated with structural alterations within the individual proteins or within the protein layer, for example loss of bindings between interacting biomolecules [71,72]. The obtained results indicate that GOx suffered more conformational changes during the immobilization process onto the ppPFM surface than onto the pgPFM surface. In fact, highly flexible domains in the GOx structure indicate that it can change to the unfolded (U) inactive state [73]. Consequently, when GOx adopt the unfolded or semi-unfolded structure an increase of the film's flexibility is observed (higher slope of the ΔD/Δf). Therefore, in the ppPFM surface there were more inactive GOx molecules than in the pgPFM surface.

Additionally, the viscoelastic properties of the ppPFM and pgPFM surfaces were determined. The thickness, viscosity and shear modulus of the final GOx layer were calculated using the Voigt model because the obtained surfaces were not rigid (D ≥ 1) (see Table 1).

As can be seen in Table 1, higher viscosity and lower shear modulus values were achieved for the GOx/pgPFM film in comparison to the GOx/ppPFM film. Thus, higher viscoelasticity was obtained using the plasma-grafting modification technique. As can be seen in Table 1, extremely high value of shear modulus for ppPFM surface was obtained. The shear modulus is related to hydration level of the surface, it increases when water content decreases [74]. Therefore, the obtained value indicates that ppPFM generates a hydrophobic environment. These results agree with the fact that PFM has hydrophobic nature [45,75], thus, the homogeneous PFM thin film obtained by plasma-polymerization gave hydrophobic properties to the surface. However, using the plasma-grafting technique PFM brushes were formed instead of a homogeneous film and the hydrophobicity of the surface was reduced (AFM and FE-SEM images can be seen in the Supplementary Materials). Therefore, pgPFM offered a more suitable microenvironment for GOx and thus, less structural changes were achieved in comparison with ppPFM. This affirmation agreed with the previous results obtained from the ΔD/Δf correlation.

Moreover, the viscoelastic properties for ppPFM film were modified after the SDS cleaning process. The thickness increased, whereas the viscosity and the shear modulus decreased. Thus, the structural conformation of GOx molecules was altered during SDS cleaning step and the initial GOx conformation was not recovered with the final PBS cleaning. On the contrary, for pgPFM film the viscoelastic properties values remained almost constant after the SDS cleaning, only the shear modulus decreased. Thus, in pgPFM, GOx was modified by the SDS solution, but finally recovered its initial conformation with the final PBS cleaning.

Table 1
Thickness, viscosity and shear modulus obtained by using Voigt model, before and after SDS was pumped into the measuring chamber. The values obtained for both modified surfaces, the ppPFM and the pgPFM, are shown. These values were obtained from two independent calculations, deviation (s) is shown.

	Surface	Thickness ± s / nm	Viscosity ± s / 10^3 Pa s^{-1}	Shear modulus ± s / 10^{-6} Pa
Before SDS	ppPFM	19.6 ± 0.3	1.29 ± 0.04	619405.0 ± 417.2
	pgPFM	16.5 ± 0.3	1.54 ± 0.01	25.3 ± 1.6
After SDS	ppPFM	47.1 ± 0.1	1.06 ± 0.01	97.3 ± 0.2
	pgPFM	15.9 ± 0.5	1.42 ± 0.02	3.2 ± 0.1

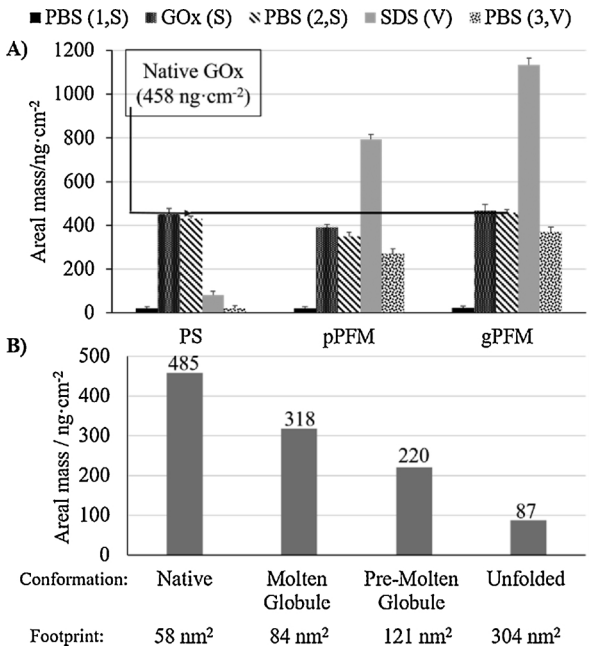

Fig. 2. A) Areal mass calculated for each individual measuring step done with the QCM-D for three different surfaces: polystyrene (PS), PFM polymerization (ppPFM) and PFM grafting (pgPFM). The values shown were obtained using two different modeling calculations: Sauerbrey (S) for rigid surfaces and Voigt (V) for flexible surfaces. These values were obtained from two independent calculations, standard deviation is shown as error bars. B) Footprint and areal mass values calculated for the native, the molten globule, the pre-molten globule and the unfolded states of GOx molecules. Values are obtained when performing calculations on a single bibliographic value.

3.3. Study of GOx conformation when immobilized on the modified surfaces

As previously mentioned, the enzyme immobilization process can cause conformational changes in the proteins structure [76]. To evaluate the structural conformation of GOx molecules once immobilized, the adsorbed mass of a protein monolayer was calculated using the GOx native structure footprint (58 nm^2) [77]. The obtained value (458 ng cm^{-2}) was compared to the real areal mass adsorbed onto the three studied surfaces for each measuring step: baseline (PBS 1), GOx immobilization, first cleaning step (PBS 2), GOx interaction with SDS and final PBS cleaning (PBS 3) (see Fig. 2.A). Two types of models were applied to obtain these results: Sauerbrey for rigid films (the initial GOx layer) and Voigt for flexible surfaces (the final protein film). Thus, ppPFM surface adsorbed 350 ng cm^{-2} of protein before the SDS cleaning whereas the pgPFM retained 458 ng cm^{-2} at the same point (Sauerbrey model). However, 271 ng cm^{-2} of protein were retained onto the final ppPFM surface, whereas the final pgPFM surface adsorbed 372 ng cm^{-2} of enzyme (Voigt model). Diminution of weight after the SDS cleaning indicates that the non-covalently attached enzyme molecules were satisfactorily removed from both surfaces.

The areal mass values obtained with the studied films were related with its corresponding thickness values (see Table 1). The highest thickness was achieved for the ppPFM film (47.1 nm) that presented the lower areal mass (271 ng cm^{-2}). The resulting pgPFM surface had a thickness of 15.9 nm and adsorbed 372 ng cm^{-2} of protein. It is known that a single protein molecule in the MG state has an average radius more than 15% in comparison with the average radius of the same

protein molecule in the native state [78]. This radius increase corresponds to a volume increase of about 50% [78]. Therefore, the obtained results allow to propose the hypothesis that in the ppPFM surface the GOx molecules adopted unfolded or semi-unfolded structures, while in the pgPFM a globular structure was achieved. Note that one single molecule of GOx had a higher area in the ppPFM film than in the pgPFM surface. Thus, there would be more adsorbed mass onto the pgPFM modified surface than onto the ppPFM surface.

To confirm which conformation adopted the GOx molecules, the theoretical areal mass for each possible structure was calculated and compared with the experimental values. As previously mentioned, globular proteins can exist at least in four different conformations: N, MG, PMG and U states [78]. On one hand, the protein in the MG is slightly opened but the globular conformation is maintained. On the other hand, the protein in the PMG losses approximately the 50% of the native-like secondary structure and the globular conformation. Moreover, the PMG state is less compact and less rigid than the MG and the N structures. It is also known that the hydrodynamic volume of the protein molecules is increased with the unfolding degree of the protein; in the MG, the PMG and the U states this parameter increases approximately 1.5, 3 and 12 times respectively in comparison to that of the N state [78]. Therefore, using the footprint of the native GOx (58 nm^2), it is possible to determine its hydrodynamic volume supposing that the protein was a sphere. And then, using the bibliographic factor for the volume increase in each state it was possible to calculate its theoretical footprints (see Fig. 2.B). Then, the areal mass adsorbed for each state was determined (see Fig. 2.B) and these values were compared with the experimental values obtained for the ppPFM and the pgPFM surfaces.

For the ppPFM surface, about 271 ng cm^{-2} was obtained using the QCM-D (Voigt calculation). This value is comprised between the theoretical values for the MG (318 ng cm^{-2}) and for the PMG (220 ng cm^{-2}) states, indicating that these two intermediates were immobilized simultaneously onto the ppPFM surface. These results agree with the previous hypothesis that no native GOx was immobilized when the plasma-polymerization was performed. On the other hand, the experimental value obtained for the pgPFM surface was 372 ng cm^{-2}. This value is comprised between the theoretical values for the N (458 ng cm^{-2}) and the MG (318 ng cm^{-2}) states. Thus, both conformations were simultaneously immobilized in the pgPFM surface.

Summarizing, the use of plasma-grafting allows to keep enzymatic activity of GOx better than the use of plasma-polymerization. For this reason, plasma-grafting modification technique was selected to develop the electrochemical platform.

3.4. Glucose biosensor development

To confirm that the pgPFM surface can be used to successfully immobilize GOx onto rigid surfaces, titanium sensors were used to reproduce the previous described QCM-D experiments onto PS. Two different surfaces were studied, non-modified titanium (Ti) and a pgPFM. It is worth mentioning that it is very difficult to obtain a plasma-grafting onto a metallic surface, where the electrons simply pass through the surface and no radicals are formed. For this reason, before the plasma-grafting modification it was necessary to introduce an organic bed onto the metal. Therefore, a homogeneous film of HEMA copolymerized with EGDA was deposited via plasma-polymerization onto the electrode. The criteria selection of HEMA was based on previous studies done by our research group [79,80]. Thin films of poly-HEMA can be used to protect electrode surfaces in biosensing applications, without interfering in the electrochemical sensor response. Moreover, the resulting hydrogel film shows high biocompatibility and offers an enzyme-friendly environment [54,81]. Thus, a Ti/HEMA-co-EGDA/pgPFM surface was obtained. In Fig. 3, changes in both frequency (f) and dissipation (D) recorded for Ti and Ti/HEMA-co-EGDA/pgPFM are shown.

Fig. 3 shows the frequency and dissipation profiles recorded for the Ti (Fig. 3.A) and the Ti/HEMA-co-EGDA/pgPFM (Fig. 3.B). Five different measuring steps were carried out, as for the PS sensors: crystal sensor stabilization with PBS, GOx immobilization, cleaning step with PBS, interaction with SDS and return to the initial conditions with PBS. When GOx was pumped in the flow module the frequency rapidly decreased and was stabilized between −20 Hz and −25 Hz for both neat Ti and Ti/HEMA-co-EGDA/pgPFM. These results agree with thus obtained for the PS sensors and indicate an increase of the absorbed mass due to an interaction between GOx and the surfaces. Then, when the cleaning step was carried out with SDS, the unbounded molecules were eliminated, and the frequency signals increased. Finally, when PBS was used to return to the initial conditions, the frequency returned to the baseline for the Ti (Fig. 3.A) as expected and it was fixed around −10 Hz for the Ti/HEMA-co-EGDA/pgPFM (Fig. 3.B) indicating a covalent interaction between GOx and the surface.

The dissipation signals recorded for each studied surface are also shown in Fig. 3. As it can be seen before the SDS interaction, a small variation in overtones' separation was obtained, indicating that a rigid protein monolayer was formed in both cases. In contrast, when SDS was pumped into the measuring chamber a variation of the overtones' separation was recorded for the Ti (Fig. 3.A) and for the Ti/HEMA-co-EGDA/pgPFM (Fig. 3.B). This variation indicates that the adsorbed films changed through the different studied steps and thus, the protein layer was modified. So, GOx suffers conformational changes during the immobilization process. These results agree with those obtained with the PS sensors.

The dissipation and frequency profiles of Ti and Ti/HEMA-co-EGDA/pgPFM surfaces were used to determine the areal mass adsorbed onto the studied surfaces for each measuring step (see Fig. 4).

In Fig. 4, the areal mass adsorbed onto the Ti and the Ti/HEMA-co-EGDA/pgPFM surfaces are shown. These results agree with those obtained for the PS sensors; before cleaning with SDS and PBS the two studied surfaces retained almost the amount of enzyme related to the native form (458 ng·cm^{-2}), and in the final step no enzyme was retained on Ti whereas the pgPFM was able to retain 324 ng·cm^{-2} of enzyme (Voigt model). This value is comprised between the theoretical values for the N (458 ng cm^{-2}) and for the MG (318 ng cm^{-2}) states. In addition, it only differs in a 12% from the value obtained with the PS/pgPFM (372 ng cm^{-2}). Therefore, the two active forms of glucose oxidase (N and MG) were immobilized onto the Ti/HEMA-co-EGDA/pgPFM, as expected. Consequently, it can be concluded that the plasma-grafting modification is reproducible for different surfaces and it can be used to immobilize GOx.

Considering the obtained results, an amperometric glucose biosensor was developed using pgPFM. For the biosensor design, TiO_2NTAs onto metallic Ti was selected as electrochemical interface. The nanotubes formation will dramatically increase the active surface area of the electrode. Therefore, a high number of enzyme molecules can be immobilized using this architecture. In addition, TiO_2NTAs provides high biocompatibility to the system, improving the long-term stability of the biosensor [47,48]. On the other hand, Chitosan hydrogel was used as physical barrier to prevent enzyme denaturalization and contributes to stabilizing the enzyme molecules [82,83].

The amperometric response of Ti/TiO_2NTAs/HEMA-co-EGDA/pgPFM/GOx/Chitosan biosensor to continuous injections of 0.25 mM glucose in 0.1 M PBS (pH 7.0) at −0.4 V vs. Ag/AgCl, was studied under a forced convection regime of the working RDE at 2000 rpm. Conventional amperometric glucose biosensors commonly work at anodic potentials to oxidize H_2O_2 to oxygen. In contrast, the constructed biosensor works at cathodic potentials to reduce the H_2O_2 to H_2O. Thus, the effect of common interfering reductive species, such as ascorbic acid or citric acid, is overcome. Fig. 5 shows the measured current over time after each glucose addition.

As can be seen in Fig. 5, the registered current after each glucose addition (0.25 mM) increased approximately 3 μA. This result indicate that the plasma-grafting was successfully applied, and the immobilized

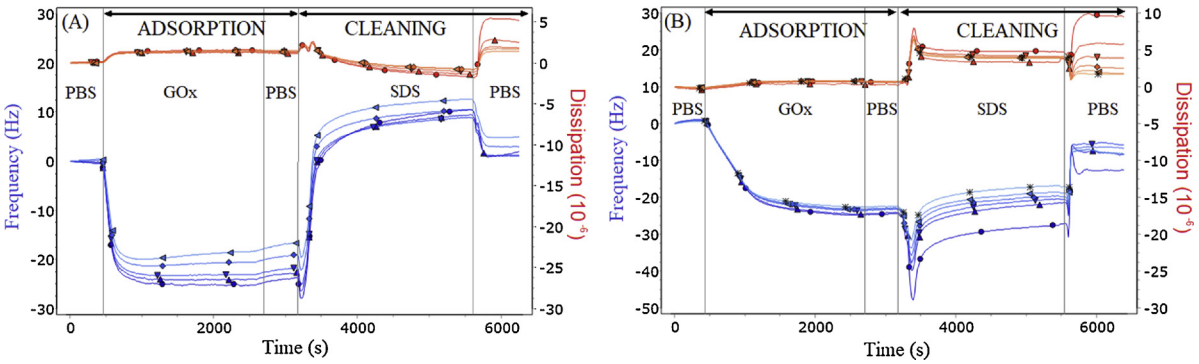

Fig. 3. Frequency (blue line) and dissipation (red line) changes with time for QCM-D monitoring of GOx immobilization and subsequent PBS and SDS cleaning on two types of surfaces: titanium (A) and plasma-grafted PFM (B). The 3rd (●), 5th (▲), 7th (▼), 9th (♦), 11th (◄) and 13th (⁎) overtones are shown (For interpretation of the references to colour in this figure legend, the reader is referred to the web version of this article).

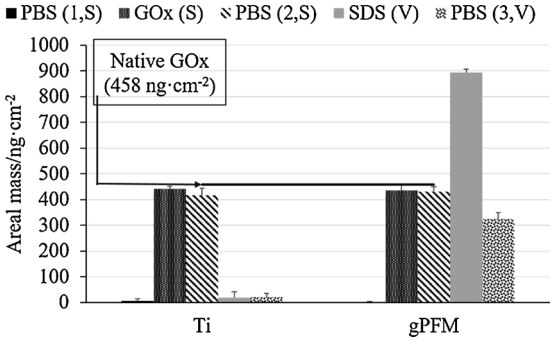

Fig. 4. Areal mass calculated for each individual measuring step done with the QCM-D for two different surfaces: titanium and PFM grafting (pgPFM). The values shown were obtained using two different modeling calculations: Sauerbrey (S) and Voigt (V). These values were obtained from two independent calculations, standard deviation is shown as error bars.

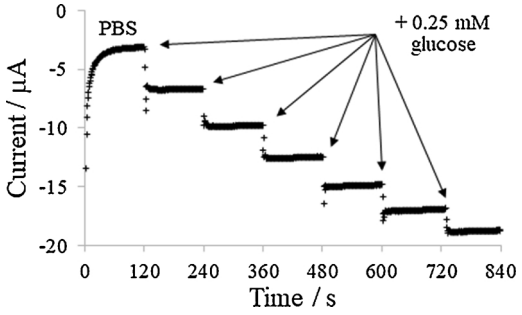

Fig. 5. Current-time plot of Ti/TiO_2NTAs/HEMA-co-EGDA/pgPFM/GOx/Chitosan biosensor with applied potential of −0.4 V vs Ag/AgCl when 0.25 mM glucose injections were done.

GOx conserve its enzymatic activity. To determine the linear range of the Ti/TiO_2NTAs/HEMA-co-EGDA/pgPFM/GOx/Chitosan biosensor, a calibration curve was built plotting the corrected current vs the glucose concentration. The corrected current was calculated as the registered current after each glucose addition minus the blank signal (PBS). The biosensor exhibited a linear range between 0.25 and 1.49 mM glucose. The linear regression equation was y (µA) = 9.76 x (mM) + 1.65, with a correlation coefficient of 0.9917. The slope of the calibration curve was associated to the biosensor sensitivity (9.76 µA·mM^{-1}) which is related to the limit of detection (LOD). The LOD was defined as the concentration that can be detected at 3 times the noise level and it was of 0.10 mM glucose. This value is in agreement with other LOD reported in literature [84,85] for other glucose biosensors. In addition, the limit of quantification (LOQ) was also calculated as the concentration that can be detected at 10 times the noise level and it was equal to 0.20 mM in glucose. Therefore, the obtained Ti/TiO_2NTAs/HEMA-co-EGDA/pgPFM electrochemical interface showed excellent analytical properties.

The Ti/TiO_2NTAs/HEMA-co-EGDA/pgPFM/GOx/Chitosan biosensor achieved a high sensitivity value (9.76 µA·mM^{-1}), in comparison to other glucose biosensors reported in literature [56,85–90]. This may result from the intrinsic structure of the proposed biosensor, where a large number of enzyme molecules were immobilized conserving its activity. TiO_2 offers excellent biocompatibility and large active surface area. The HEMA-co-EGDA hydrogel protects the electrode surface and generate a polymeric network with small mesh size that blocks large interfering molecules [79]. The PFM plasma-grafting modification guarantee that enzyme molecules were immobilized in an active conformation. And Chitosan prevents enzyme denaturalization, offering an enzyme-friendly environment. Therefore, high electrochemical activity was achieved due to the synergy of the electrochemical interface, the immobilization technique and the protection matrix.

3.5. Measurement of glucose in food samples

To corroborate the Ti/TiO_2NTAs/HEMA-co-EGDA/pgPFM/GOx/Chitosan applicability, it was used to determine the glucose concentration in four different alimentary products: soft drinks, soy sauces, tomato sauces and dairy products. These sample matrices were selected to overcome main quantification problems in classical techniques, such as HPLC. The glucose concentration of the selected samples was also determined by HPLC and the values obtained were considered as reference values. Glucose was determined by performing 2 replicate measurements by HPLC method and 3 replicate measurements using the developed biosensor. The obtained glucose concentration values with both analytical techniques and their standard deviations (s) are shown in Table 2. The variation between methods is also included in the table.

As can be seen in Table 2, the glucose content of 16 different food samples with complex matrices was determined with sufficient precision using the Ti/TiO_2NTAs/HEMA-co-EGDA/pgPFM/GOx/Chitosan biosensor. These results were compared with those obtained by the HPLC method and high correlation between methods was observed. In all the cases, the deviation was smaller than 10%. Thus, the biosensor was able to overcome all possible interferences in the selected samples. Moreover, the deviation values were smaller than most of the reported values in literature [91–94] which usually are equal or higher than 10%. Therefore, the obtained electrochemical device showed outstanding analytical properties and can be used to measure glucose in complex matrices of foodstuff with enough precision.

Summarizing, the plasma-grafting modification technique has been proven to be a useful tool to covalently immobilize enzyme molecules

Table 2
Determination of glucose in real food samples using the Ti/TiO_2NTAs/HEMA-co-EGDA/pgPFM/GOx/Chitosan biosensor and a reference HPLC method. Glucose concentration values and standard deviation (s) are shown. The deviation between both methods is also shown.

Type of Sample	Sample	$[Glucose]_{biosensor} \pm s$ / M	$[Glucose]_{HPLC} \pm s$ / M	Deviation/%
Soft drinks	D1 Orange	0.261 ± 0.008	0.251 ± 0.001	4.2
	D2 Orange	0.226 ± 0.011	0.224 ± 0.002	1.1
	D3 Orange	0.210 ± 0.009	0.209 ± 0.001	0.5
	D4 Lemon	0.207 ± 0.005	0.189 ± 0.001	9.6
	D5 Cola	0.156 ± 0.005	0.152 ± 0.001	2.5
Fried tomato	T1	0.108 ± 0.005	0.111 ± 0.003	−3.1
	T2	0.094 ± 0.003	0.088 ± 0.001	7.1
Soy sauces	S1	0.095 ± 0.001	0.090 ± 0.001	5.2
	S2	0.250 ± 0.003	0.253 ± 0.009	−1.4
Dairy products	L1 Milk	0.144 ± 0.005	0.134 ± 0.001	7.4
	L2 Yoghurt	0.144 ± 0.001	0.138 ± 0.001	4.5
	L3 Yoghurt	0.129 ± 0.003	0.119 ± 0.001	8.6
	L4 Milkshake	0.086 ± 0.002	0.079 ± 0.001	9.1
	L5 Milkshake	0.162 ± 0.011	0.160 ± 0.001	1.3
	L6 Custard	0.084 ± 0.001	0.077 ± 0.001	9.4
	L7 Caesar sauce	0.040 ± 0.002	0.037 ± 0.003	7.9

onto rigid surfaces for biosensing applications. The obtained covalent configuration allows to immobilize a large number of active enzyme molecules and to achieve high long-term stability. In addition, TiO_2 has catalytic activity through H_2O_2 reduction. Thus, the biosensor working principle is follow the hydrogen peroxide reduction using a cathodic potential instead of applying anodic potentials to oxidize this H_2O_2 to oxygen as commonly conventional amperometric biosensors do. Therefore, most common interfering reductive species such as ascorbic acid are eliminated, and high selectivity is achieved. Moreover, the resulting biosensor had great potential for practical applications; the biocompatibility and non-toxicity of its components, make the obtained interface as a suitable platform for implantable devices. Despite all the advantages of the proposed biosensor, it also has some disadvantage; the fabrication process includes a complex step of surface modification that requires sophisticated plasma techniques.

4. Conclusions

A novel and versatile electrochemical platform for biosensing applications was designed and constructed. This platform consists on a novel grafted PFM surface onto a tailored HEMA hydrogel coating in TiO_2NTAs. Glucose oxidase was used to demonstrate the high potential of the constructed electrochemical platform. It was demonstrated, using QCM-D, that the obtained pgPFM surface was able to immobilize GOx molecules mostly in its biologically active conformation. It is also worth mentioning, that the architecture of the resulting biosensor offers an enzyme friendly environment in which deactivation is prevented. This architecture, PFM grafted electrochemical interface, can be considered as an exceptional tool for the fast and accurate determination of many different analytes.

For analytical purposes, an electrochemical biosensor based on GOx was constructed using the above mentioned electrochemical platform. High sensitivity values, wide linear range and low LOD and LOQ were obtained in the calibration process. Finally, this enzymatic biosensor was used to determine the glucose content of different complex food matrices. The obtained results showed good precision in comparison to their respective HPLC values.

Since the immobilization process consists of an amide bond formation, many different enzymes can be attached onto the tailored electrochemical platform. Thus, it is possible to quantify different analytes in complex matrices just by changing the attached enzyme. Therefore, the developed interface can be considered as a selective, low power, simple and rapid alternative tool to classical analytical methods in many industrial sectors.

Author contributions

The manuscript was written through contributions of all authors. All authors have given approval to the final version of the manuscript.

Funding sources

This research did not receive any specific grant from funding agencies in the public, commercial or not-for-profit sectors.

Conflict of interest

The authors declare no competing financial interest.

Acknowledgment

The authors wish to thank Francesc Broto from Institut Químic de Sarrià for the HPLC analysis.

Appendix A. Supplementary data

Supplementary material related to this article can be found, in the online version, at doi:https://doi.org/10.1016/j.colsurfb.2018.11.076.

References

[1] E.-H. Yoo, S.-Y. Lee, Glucose biosensors: an overview of use in clinical practice, Sensors 10 (2010) 4558–4576, https://doi.org/10.3390/s100504558.
[2] M.A. Zia, A. Riaz, S. Rasul, R.Z. Abbas, Evaluation of antimicrobial activity of glucose oxidase from Aspergillus niger EBL-A and Penicillium notatum, Braz. Arch. Biol. Technol. 56 (2013) 956–961, https://doi.org/10.1590/S1516-89132013005000010.
[3] M.I. Prodromidis, M.I. Karayannis, Enzyme based amperometric biosensors for food analysis, Electroanalysis 14 (2002) 241–261, https://doi.org/10.1002/1521-4109(200202)14:4<241::AID-ELAN241>3.0.CO;2-P.
[4] C.M. Wong, K.H. Wong, X.D. Chen, Glucose oxidase: natural occurrence, function, properties and industrial applications, Appl. Microbiol. Biotechnol. 78 (2008) 927–938, https://doi.org/10.1007/s00253-008-1407-4.
[5] B. Dhar Malhotra, C. Mouli Pandey, Biosensors: Fundamentals and Applications, first edit, Smithers Rapra Technology Ltd, Shawbury, 2017.
[6] D. Grieshaber, R. MacKenzie, J. Vörös, E. Reimhult, Electrochemical biosensors - sensor principles and architectures, Sensors 8 (2008) 1400–1458, https://doi.org/10.3390/s80314000.
[7] X. Wang, S.V. Dzyadevych, J.M. Chovelon, N.J. Renault, L. Chen, S. Xia, J. Zhao, Development of a conductometric nitrate biosensor based on Methyl viologen/Nafion® composite film, Electrochem. Commun. 8 (2006) 201–205, https://doi.org/10.1016/j.elecom.2005.11.006.
[8] O.V. Soldatkina, O.O. Soldatkin, T.P. Velychko, V.O. Prilipko, M.A. Kuibida, S.V. Dzyadevych, Conductometric biosensor for arginine determination in pharmaceutics, Bioelectrochemistry 124 (2018) 40–46, https://doi.org/10.1016/j.bioelechem.2018.07.002.
[9] C.Y.(Kevin) Lai, P.J.S. Foot, J.W. Brown, P. Spearman, A urea potentiometric

biosensor based on a thiophene copolymer, Biosensors 7 (2017) 1–13, https://doi.org/10.3390/bios7010013.
[10] P.F. Draghi, J.C.B. Fernandes, Label-free potentiometric biosensor based on solid-contact for determination of total phenols in honey and propolis, Talanta 164 (2017) 413–417, https://doi.org/10.1016/j.talanta.2016.12.002.
[11] H. Kaur, S. Kumar, N. Verma, Enzyme-based colorimetric and potentiometric biosensor for detecting Pb (II) ions in milk, Braz. Arch. Biol. Technol. 57 (2014) 613–619, https://doi.org/10.1590/S1516-8913201402160.
[12] M. Pohanka, P. Skládal, Electrochemical biosensors – principles and applications, J. Appl. Biomed. 6 (2008) 57–64.
[13] M. Portaccio, D. Di Tuoro, F. Arduini, M. Lepore, D.G. Mita, N. Diano, L. Mita, D. Moscone, A thionine-modified carbon paste amperometric biosensor for catechol and bisphenol A determination, Biosens. Bioelectron. 25 (2010) 2003–2008, https://doi.org/10.1016/j.bios.2010.01.025.
[14] R.C.H. Kwan, C. Chan, R. Renneberg, An amperometric biosensor for determining amino acids using a bienzymatic system containing amino acid oxidase and protease, Biotechnol. Lett. 24 (2002) 1203–1207, https://doi.org/10.1023/A:1016163315804.
[15] F. Conzuelo, M. Gamella, S. Campuzano, M.A. Ruiz, A.J. Reviejo, J.M. Pingarrón, An integrated amperometric biosensor for the determination of lactose in milk and dairy products, J. Agric. Food Chem. 58 (2010) 7141–7148, https://doi.org/10.1021/jf101173e.
[16] W. Dungchai, W. Siangproh, W. Chaicumpa, P. Tongtawe, O. Chailapakul, Salmonella typhi determination using voltammetric amplification of nanoparticles: a highly sensitive strategy for metalloimmunoassay based on a copper-enhanced gold label, Talanta. 77 (2008) 727–732, https://doi.org/10.1016/j.talanta.2008.07.014.
[17] F.T.C. Moreira, M.G.F. Sale, M. Di Lorenzo, Towards timely Alzheimer diagnosis: a self-powered amperometric biosensor for the neurotransmitter acetylcholine, Biosens. Bioelectron. 87 (2017) 607–614, https://doi.org/10.1016/j.bios.2016.08.104.
[18] L.C. Clark, C. Lyons, Electrode systems for continuous monitoring in cardiovascular surgery, Ann. N. Y. Acad. Sci. 102 (1962) 29–45.
[19] A.P.F. Turner, Biosensors: sense and sensibility, Chem. Soc. Rev. 43 (2013) 3184, https://doi.org/10.1039/c3cs35528d.
[20] P. Bollella, L. Gorton, R. Ludwig, R. Antiochia, A third generation glucose biosensor based on cellobiose dehydrogenase immobilized on a glassy carbon electrode decorated with electrodeposited gold nanoparticles: characterization and application in human saliva, Sensors 17 (2017) 1912, https://doi.org/10.3390/s17081912.
[21] P. Rafighi, M. Tavahodi, B. Haghighi, Fabrication of a third-generation glucose biosensor using graphene-polyethyleneimine-gold nanoparticles hybrid, Sens. Actuators B Chem. 232 (2016) 454–461, https://doi.org/10.1016/j.snb.2016.03.147.
[22] I. Taurino, G. Sanzò, R. Antiochia, C. Tortolini, F. Mazzei, G. Favero, G. De Micheli, S. Carrara, Recent advances in third generation biosensors based on Au and Pt nanostructured electrodes, TrAC Trends Anal. Chem. 79 (2016) 151–159, https://doi.org/10.1016/j.trac.2016.01.020.
[23] Z. Chu, Y. Liu, Y. Xu, L. Shi, J. Peng, W. Jin, In-situ fabrication of well-distributed gold nanocubes on thiol graphene as a third-generation biosensor for ultrasensitive glucose detection, Electrochim. Acta 176 (2015) 162–171, https://doi.org/10.1016/j.electacta.2015.06.123.
[24] E. Mehmeti, D.M. Stanković, S. Chaiyo, J. Zavasnik, K. Žagar, K. Kalcher, Wiring of glucose oxidase with graphene nanoribbons: an electrochemical third generation glucose biosensor, Microchim. Acta. 184 (2017) 1127–1134, https://doi.org/10.1007/s00604-017-2115-5.
[25] M. Marquitan, T. Bobrowski, A. Ernst, P. Wilde, J. Clausmeyer, A. Ruff, W. Schuhmann, Miniaturized amperometric glucose sensors based on polymer/enzyme modified carbon electrodes in the sub-micrometer scale, J. Electrochem. Soc. 165 (2018) G3008–G3014, https://doi.org/10.1149/2.0021812jes.
[26] F. Ribet, G. Stemme, N. Roxhed, Ultra-miniaturization of a planar amperometric sensor targeting continuous intradermal glucose monitoring, Biosens. Bioelectron. 90 (2017) 577–583, https://doi.org/10.1016/j.bios.2016.10.007.
[27] C. Ziller, J. Lin, P. Knittel, L. Friedrich, C. Andronescu, S. Pöller, W. Schuhmann, C. Kranz, Poly(benzoxazine) as an immobilization matrix for miniaturized ATP and glucose biosensors, ChemElectroChem 4 (2017) 864–871, https://doi.org/10.1002/celc.201600765.
[28] G. Hughes, R.M. Pemberton, P. Nicholas, J.P. Hart, Fabrication of miniaturised screen-printed glucose biosensors, using a water-based ink, and the evaluation of their electrochemical behaviour, Electroanalysis 30 (2018) 1616–1620, https://doi.org/10.1002/elan.201800104.
[29] A. Soni, S.K. Jha, A paper strip based non-invasive glucose biosensor for salivary analysis, Biosens. Bioelectron. 67 (2015) 763–768, https://doi.org/10.1016/j.bios.2014.09.042.
[30] L. Lipani, B.G.R. Dupont, F. Doungmene, F. Marken, R.M. Tyrrell, R.H. Guy, A. Ilie, Non-invasive, transdermal, path-selective and specific glucose monitoring via a graphene-based platform, Nat. Nanotechnol. 13 (2018) 504–511, https://doi.org/10.1038/s41565-018-0112-4.
[31] A.J. Bandodkar, J. Wang, Non-invasive wearable electrochemical sensors: a review, Trends Biotechnol. 32 (2014) 363–371, https://doi.org/10.1016/j.tibtech.2014.04.005.
[32] A. Soni, S.K. Jha, Smartphone based non-invasive salivary glucose biosensor, Anal. Chim. Acta 996 (2017) 54–63, https://doi.org/10.1016/j.aca.2017.10.003.
[33] K. Sun, Y. Yang, H. Zhou, S. Yin, W. Qin, J. Yu, D.T. Chiu, Z. Yuan, X. Zhang, C. Wu, Ultrabright polymer-dot transducer enabled wireless glucose monitoring via a smartphone, ACS Nano 12 (2018) 5176–5184, https://doi.org/10.1021/acsnano.8b02188.
[34] M. Elsherif, M.U. Hassan, A.K. Yetisen, H. Butt, Wearable contact Lens biosensors for continuous glucose monitoring using smartphones, ACS Nano 12 (2018) 5452–5462, https://doi.org/10.1021/acsnano.8b00829.
[35] A. Sassolas, L.J. Blum, B.D. Leca-Bouvier, Immobilization strategies to develop enzymatic biosensors, Biotechnol. Adv. 30 (2012) 489–511, https://doi.org/10.1016/j.biotechadv.2011.09.003.
[36] P. Ciaurriz, E. Bravo, K. Hamad-Schifferli, Effect of architecture on the activity of glucose oxidase/horseradish peroxidase/carbon nanoparticle conjugates, J. Colloid Interface Sci. 414 (2014) 73–81, https://doi.org/10.1016/j.jcis.2013.09.039.
[37] P. Fabry, J. Fouletier, Amperometric sensors, Chem. Biol. Microsens. Appl. Fluid Media, Wiley-ISTE, 2009, pp. 115–171.
[38] S. Ferri, K. Kojima, K. Sode, Review of glucose oxidases and glucose dehydrogenases: a bird's eye view of glucose sensing enzymes, J. Diabetes Sci. Technol. 5 (2011) 1068–1076, https://doi.org/10.1177/193229681100500507.
[39] B. Mecheri, D. De Porcellinis, P.T. Campana, A. Rainer, M. Trombetta, A. Marletta, O.N. Oliveira, S. Licoccia, Tuning structural changes in glucose oxidase for enzyme fuel cell applications, ACS Appl. Mater. Interfaces 7 (2015) 28311–28318, https://doi.org/10.1021/acsami.5b08610.
[40] L. Francesch, S. Borros, W. Knoll, R. Förch, Surface reactivity of pulsed-plasma polymerized pentafluorophenyl methacrylate (PFM) toward amines and proteins in solution, Langmuir 23 (2007) 3927–3931, https://doi.org/10.1021/la062422d.
[41] E. Wijaya, C. Lenaerts, S. Maricot, J. Hastanin, S. Habraken, J.P. Vilcot, R. Boukherroub, S. Szunerits, Surface plasmon resonance-based biosensors: from the development of different SPR structures to novel surface functionalization strategies, Curr. Opin. Solid State Mater. Sci. 15 (2011) 208–224, https://doi.org/10.1016/j.cossms.2011.05.001.
[42] A. Cifuentes-Rius, A. de Pablo, V. Ramos-Perez, S. Borros, Tailoring carbon nanotubes surface for gene delivery applications, Plasma Process. Polym. 11 (2014) 704–713, https://doi.org/10.1002/ppap.201300167.
[43] A. Cifuentes, S. Borrós, Comparison of two different plasma surface-modification techniques for the covalent immobilization of protein monolayers, Langmuir. 29 (2013) 6645–6651, https://doi.org/10.1021/la400597e.
[44] D. Horna, J.C. Ramírez, A. Cifuentes, A. Bernad, S. Borrós, M.A. González, Efficient cell reprogramming using bioengineered surfaces, Adv. Healthc. Mater. 1 (2012) 177–182, https://doi.org/10.1002/adhm.201200017.
[45] L. Duque, N. Queralto, L. Francesch, G.G. Bumbu, S. Borros, R. Berger, R. Förch, Reactions of plasma-polymerised pentafluorophenyl methacrylate with simple amines, Plasma Process. Polym. 7 (2010) 915–925, https://doi.org/10.1002/ppap.201000058.
[46] J. Wang, Nanomaterial-based electrochemical biosensors, Analyst 130 (2005) 421, https://doi.org/10.1039/b414248a.
[47] C. Feng, G. Xu, H. Liu, J. Lv, Z. Zheng, Y. Wu, Glucose biosensors based on Ag nanoparticles modified TiO2 nanotube arrays, J. Solid State Electrochem. (2013), https://doi.org/10.1007/s10008-013-2257-2.
[48] S. Yoriya, C. a Grimes, Self-assembled TiO(2) nanotube arrays by anodization of titanium in diethylene glycol: approach to extended pore widening, Langmuir 26 (2010) 417–420, https://doi.org/10.1021/la9020146.
[49] J. Zhu, X. Liu, X. Wang, X. Huo, R. Yan, Preparation of polyaniline–TiO2 nanotube composite for the development of electrochemical biosensors, Sens. Actuators B Chem. 221 (2015) 450–457, https://doi.org/10.1016/j.snb.2015.06.131.
[50] W. Tang, L. Li, X. Zeng, A glucose biosensor based on the synergistic action of nanometer-sized TiO2 and polyaniline, Talanta 131 (2015) 417–423, https://doi.org/10.1016/j.talanta.2014.08.019.
[51] X. Chen, G. Li, G. Zhang, K. Hou, H. Pan, M. Du, Self-assembly of palladium nanoparticles on functional TiO2 nanotubes for a nonenzymatic glucose sensor, Mater. Sci. Eng. C. 62 (2016) 323–328, https://doi.org/10.1016/j.msec.2016.01.068.
[52] G.G. Bessegato, F.F. Hudari, M.V.B. Zanoni, Self-doped TiO2 nanotube electrodes: a powerful tool as a sensor platform for electroanalytical applications, Electrochim. Acta 235 (2017) 527–533, https://doi.org/10.1016/j.electacta.2017.03.141.
[53] L. Duque, B. Menges, S. Borros, R. Förch, Immobilization of biomolecules to plasma polymerized pentafluorophenyl methacrylate, Biomacromolecules 11 (2010) 2818–2823, https://doi.org/10.1021/bm100910q.
[54] L. Montero, S.H. Baxamusa, S. Borros, K.K. Gleason, Thin hydrogel films with nanoconfined surface reactivity by photoinitiated chemical vapor deposition, Chem. Mater. 21 (2009) 399–403, https://doi.org/10.1021/cm802737m.
[55] J. Gilabert-Porres, S. Martí, L. Calatayud, V. Ramos, A. Rosell, S. Borrós, Design of a nanostructured active surface against gram-positive and gram-negative Bacteria through plasma activation and in situ silver reduction, ACS Appl. Mater. Interfaces 8 (2016) 64–73, https://doi.org/10.1021/acsami.5b07115.
[56] M. Artigues, J. Abellà, S. Colominas, Analytical parameters of an amperometric glucose biosensor for fast analysis in food samples, Sensors 17 (2017) 2620, https://doi.org/10.3390/s17112620.
[57] AOAC, Official method 977.20: separation of sugars in honey, liquid chromatographic method, JAOAC 60 (1977) 838.
[58] P. Shanmugavelan, S.Y. Kim, J.B. Kim, H.W. Kim, S.M. Cho, S.N. Kim, S.Y. Kim, Y.S. Cho, H.R. Kim, Evaluation of sugar content and composition in commonly consumed Korean vegetables, fruits, cereals, seed plants, and leaves by HPLC-ELSD, Carbohydr. Res. 380 (2013) 112–117, https://doi.org/10.1016/j.carres.2013.06.024.
[59] J.M. Langemeier, D.E. Rogers, Rapid method for sugar analysis of doughs and baked products, Cereal Chem. 72 (1995) 349–351.
[60] S. Sungur, Y. Kilboz, Determination of sugar profiles of sweetened foods and beverages, J. Food Nutr. Res. 4 (2016) 349–354, https://doi.org/10.12691/jfnr-4-6-2.
[61] AOAC, Official Method 982.14: Glucose, Fructose, Sucrose, and Maltose in Presweetened Cereals, (1990).
[62] AOAC, Official Method 980.13: Fructose, Glucose, Lactose, Maltose, Sucrose in Milk

Chocolate, (1990).
[63] M.N. Jones, P. Manley, A. Wilkinson, The dissociation of glucose oxidase by sodium n-dodecyl sulphate, Biochem. J. 203 (1982) 285–291.
[64] S. Borrós, S. Oh, M. Wilcox, J.P. Pearson, Optimal design for studying mucoadhesive polymers interaction with gastric mucin using a quartz crystal microbalance with dissipation (QCM-D): Comparison of two different mucin origins, Eur. J. Pharm. Biopharm. 96 (2015) 477–483, https://doi.org/10.1016/j.ejpb.2015.08.002.
[65] S. Khatun Haq, M. Faiz Ahmad, R. Hasan Khan, The acid-induced state of glucose oxidase exists as a compact folded intermediate, Biochem. Biophys. Res. Commun. 303 (2003) 685–692, https://doi.org/10.1016/S0006-291X(03)00383-8.
[66] M. Ohgushi, A. Wada, "Molten-globule state": a compact form of globular proteins with mobile side-chains, FEBS Lett. 164 (1983) 21–24, https://doi.org/10.1016/0014-5793(83)80010-6.
[67] L. Dumitraşcu, N. Stănciuc, G.E. Bahrim, A. Ciumac, I. Aprodu, pH and heat-dependent behaviour of glucose oxidase down to single molecule level by combined fluorescence spectroscopy and molecular modelling, J. Sci. Food Agric. 96 (2016) 1906–1914, https://doi.org/10.1002/jsfa.7296.
[68] V.N. Uversky, O.B. Ptitsyn, Further evidence on the equilibrium "pre-molten globule state": four-state guanidinium chloride-induced unfolding of carbonic anhydrase B at low temperature, J. Mol. Biol. 255 (1996) 215–228, https://doi.org/10.1006/jmbi.1996.0018.
[69] A.F. Chaffotte, J.I. Guijarro, Y. Guillou, M. Delepierre, M.E. Goldberg, The "pre-molten globule", a new intermediate in protein folding, J. Protein Chem. 16 (1997) 433–439.
[70] A.A. Feiler, A. Sahlholm, T. Sandberg, K.D. Caldwell, Adsorption and viscoelastic properties of fractionated mucin (BSM) and bovine serum albumin (BSA) studied with quartz crystal microbalance (QCM-D), J. Colloid Interface Sci. 315 (2007) 475–481, https://doi.org/10.1016/j.jcis.2007.07.029.
[71] F. Höök, M. Rodahl, P. Brezezinski, B. Kasemo, Energy dissipation kinetics for protein and antibody - antigen adsorption under shear oscillation on a quartz crystal microbalance, Langmuir 14 (1998) 729–734, https://doi.org/10.1021/la970815u.
[72] F. Hak, M. Rodahl, B. Kasemo, P. Brzezinski, Structural changes in hemoglobin during adsorption to solid surfaces: effects of pH, ionic strength, and ligand binding, Proc. Natl. Acad. Sci. U. S. A. 95 (1998) 12271–12276, https://doi.org/10.1073/pnas.95.21.12271.
[73] F. Janati-Fard, M.R. Housaindokht, H. Monhemi, Investigation of structural stability and enzymatic activity of glucose oxidase and its subunits, J. Mol. Catal., B Enzym. 134 (2016) 16–24, https://doi.org/10.1016/j.molcatb.2016.09.008.
[74] G.V. Lubarsky, M.R. Davidson, R.H. Bradley, Hydration-dehydration of adsorbed protein films studied by AFM and QCM-D, Biosens. Bioelectron. 22 (2007) 1275–1281, https://doi.org/10.1016/j.bios.2006.05.024.
[75] L. Francesch, E. Garreta, M. Balcells, E.R. Edelman, S. Borrós, Fabrication of bioactive surfaces by plasma polymerization techniques using a novel acrylate-derived monomer, Plasma Process. Polym. 2 (2005) 605–611, https://doi.org/10.1002/ppap.200500042.
[76] U.B. Jensen, E.E. Ferapontova, D.S. Sutherland, Quantifying protein adsorption and function at nanostructured materials: enzymatic activity of glucose oxidase at GLAD structured electrodes, Langmuir 28 (2012) 11106–11114, https://doi.org/10.1021/la3017672.
[77] M. Gamella, N. Guz, S. Mailloux, J.M. Pingarrón, E. Katz, Activation of a biocatalytic electrode by removing glucose oxidase from the surface-application to signal triggered drug release, ACS Appl. Mater. Interfaces 6 (2014) 13349–13354, https://doi.org/10.1021/am504561d.
[78] V.N. Uversky, Natively unfolded proteins: a point where biology waits for physics, Protein Sci. 11 (2002) 739–756, https://doi.org/10.1110/ps.4210102.matic.
[79] S.H. Baxamusa, L. Montero, J.M. Dubach, H.A. Clark, S. Borros, K.K. Gleason, Protection of sensors for biological applications by photoinitiated chemical vapor deposition of hydrogel thin films, Biomacromolecules 9 (2008) 2857–2862, https://doi.org/10.1021/bm800632d.
[80] L. Montero, G. Gabriel, A. Guimerà, R. Villa, K.K. Gleason, Increasing biosensor response through hydrogel thin fi lm deposition : influence of hydrogel thickness, Vacuum 86 (2012) 2102–2104, https://doi.org/10.1016/j.vacuum.2012.06.002.
[81] N. Marí-Buyé, S. O'Shaughnessy, C. Colominas, C.E. Semino, K.K. Gleason, S. Borrós, Functionalized, swellable hydrogel layers as a platform for cell studies, Adv. Funct. Mater. 19 (2009) 1–11, https://doi.org/10.1002/adfm.200801561.
[82] B. Krajewska, Application of chitin- and chitosan-based materials for enzyme immobilizations: a review, Enzyme Microb. Technol. 35 (2004) 126–139, https://doi.org/10.1016/j.enzmictec.2003.12.013.
[83] G. Hughes, R.M. Pemberton, P.R. Fielden, J.P. Hart, The design, development and application of electrochemical glutamate biosensors, Trends Analyt. Chem. 79 (2015) 106–113, https://doi.org/10.1016/j.trac.2015.10.020.
[84] Q. Kang, L. Yang, Q. Cai, An electro-catalytic biosensor fabricated with Pt-Au nanoparticle-decorated titania nanotube array, Bioelectrochemistry 74 (2008) 62–65, https://doi.org/10.1016/j.bioelechem.2008.06.004.
[85] F.Y. Kong, S.X. Gu, W.W. Li, T.T. Chen, Q. Xu, W. Wang, A paper disk equipped with graphene/polyaniline/Au nanoparticles/glucose oxidase biocomposite modified screen-printed electrode: toward whole blood glucose determination, Biosens. Bioelectron. 56 (2014) 77–82, https://doi.org/10.1016/j.bios.2013.12.067.
[86] N. Chandra Sekar, S.A. Mousavi Shaegh, S.H. Ng, L. Ge, S.N. Tan, A paper-based amperometric glucose biosensor developed with Prussian Blue-modified screen-printed electrodes, Sens. Actuators, B Chem. 204 (2014) 414–420, https://doi.org/10.1016/j.snb.2014.07.103.
[87] C. Esmaeili, M. Abdi, A. Mathew, M. Jonoobi, K. Oksman, M. Rezayi, Synergy effect of nanocrystalline cellulose for the biosensing detection of glucose, Sensors. 15 (2015) 24681–24697, https://doi.org/10.3390/s151024681.
[88] Y. Lin, L. Hu, L. Yin, L. Guo, Electrochemical glucose biosensor with improved performance based on the use of glucose oxidase and Prussian Blue incorporated into a thin film of self-polymerized dopamine, Sens. Actuators, B Chem. 210 (2015) 513–518, https://doi.org/10.1016/j.snb.2014.12.107.
[89] X. Shen, X. Xia, Y. Du, W. Ye, C. Wang, Amperometric glucose biosensor based on AuPd modified reduced graphene oxide/polyimide film with glucose oxidase, J. Electrochem. Soc. 164 (2017) B285–B291, https://doi.org/10.1149/2.1591706jes.
[90] A. Jędrzak, T. Rębiś, Ł. Klapiszewski, J. Zdarta, G. Milczarek, T. Jesionowski, Carbon paste electrode based on functional GOx/silica-lignin system to prepare an amperometric glucose biosensor, Sens. Actuators B Chem. 256 (2018) 176–185, https://doi.org/10.1016/j.snb.2017.10.079.
[91] S. Campuzano, O.A. Loaiza, M. Pedrero, F.J.M. de Villena, J.M. Pingarrón, An integrated bienzyme glucose oxidase-fructose dehydrogenase-tetrathiafulvalene-3-mercaptopropionic acid-gold electrode for the simultaneous determination of glucose and fructose, Bioelectrochemistry 63 (2004) 199–206, https://doi.org/10.1016/j.bioelechem.2003.10.019.
[92] T.B. Goriushkina, A.P. Soldatkin, S.V. Dzyadevych, Application of amperometric biosensors for analysis of ethanol, glucose, and lactate in wine, J. Agric. Food Chem. 57 (2009) 6528–6535, https://doi.org/10.1021/jf9009087.
[93] D. Albanese, A. Sannini, F. Malvano, R. Pilloton, M. Di Matteo, Optimisation of glucose biosensors based on sol-gel entrapment and Prussian blue-modified screen-printed electrodes for real food analysis, Food Anal. Methods 7 (2014) 1002–1008, https://doi.org/10.1007/s12161-013-9705-6.
[94] M. Ammam, J. Fransaer, Two-enzyme lactose biosensor based on β-galactosidase and glucose oxidase deposited by AC-electrophoresis: characteristics and performance for lactose determination in milk, Sens. Actuators B Chem. 148 (2010) 583–589, https://doi.org/10.1016/j.snb.2010.05.027.